The Korean Journal of Rheology,
Vol. 5, No. 1, June 1993 pp.23-33

〈연구논문〉

폴리에틸렌과 나일론6의 비상용 블렌드의 유변학적 · 형태학적 특성에 관한 연구

최수명 · 홍성일*

동양나이론 중앙연구소, *서울대학교 공과대학 섬유고분자공학과

(1993년 2월 23일 접수)

A Study on the Rheological and Morphological Properties for Immiscible Blends of Polyethylene and Nylon 6

Soo Myung Choi and Sung Il Hong*

R&D Center Tong Yang Nylon Co., Ltd., Anyang 430-080, Korea
*Department of Fiber and Polymer Science, Seoul National University, Seoul 151-742, Korea

(Received February 23, 1993)

요 약

저밀도폴리에틸렌과 나일론6의 블렌드가 용융압출기의 사용에 의해 제조되었다. 제조된 비상용 블렌드의 유변학적, 형태학적 분석을 통하여 이들 사이의 상관관계를 조사하였다. 전단속도, 계면장력, 용융점도, 분산상의 농도들에 대한 분산상의 크기의 의존성을 평가하였다. 한편, 신장유동에 의한 모폴로지 변화를 조사하기 위하여 기제조된 블렌드를 사용하여 용융방사를 하였다. 이러한 방사실험으로부터 본 연구에 사용된 저밀도 폴리에틸렌과 나일론6는 분산상과 연속상의 신장점도의 상대적 크기에 무관하게 피브릴화가 되어, 방사 연신비의 증가에 의해 매우 가는 분산된 피브릴을 얻을 수 있었다.

Abstract—Blends of low density polyethylene and nylon 6 were prepared in a screw extruder combined with a static mixer. These immiscible binary blends were investigated considering the rheological properties and phase morphology. The effect of hydrodynamic conditions such as shear rate, interfacial tension, viscosity, and dispersed phase concentration on the number average size of the dispersed phase was studied. In order to study morphological changes in the fiber cross-section during the attenuation process of the fiber, an experiment by a lab-scale melt spinning equipment was carried out. The dispersed fibrils of nylon 6 or LDPE could be made much thinner by increasing the stretch ratio, irrespective of elongational viscosity ratio of the dispersed to continuous phases.

Keywords: Dispersed phase, Continuous phase, Shear viscosity, Interfacial tension, Elongational viscosity, Fibrillation

1. Introduction

Immiscible blends have distinct potential advantages because of their characteristic features. They form a multi-phase system with a deformable minor phase, and under the appropriate conditions morphological structures such as spheres, ellipsoids, fibers and plates or ribbons can be produced. Co-continuous phases may also be formed. In a suspension or emulsion of a liquid drop in

a continuous phase fluid under steady or in an extensional flow field, the liquid drop will be deformed due to the viscous (and possibly elastic) stresses acting on the interface of the drop. The interfacial tension will tend to resist the defromation and keep the drop in a spherical form.

Up to date, most studies have been limited to Newtonian systems. The first such work was done by Taylor [1, 2]. This work provided the basis for more extensive studies which followed by Bartok and Mason [3, 4], Rumscheidt and Mason [5, 6], and Karam and Bellinger [7]. Similarly, such studies have been used to describe the flow behavior of polymer solutions and melts [8, 9].

As will be shown, the breakup characteristics in viscoelastic systems can be quite different from those in Newtonian systems. With viscoelastic systems the deformation variables and the orientation angle can not be represented strictly in terms of a Weber group and a viscosity ratio group as with Newtonian systems. Additional groups should be considered as a result of the more complicated rheological properties of the viscoelastic phase. For a viscoelastic drop in a Newtonian continuous phase or for a Newtonian drop in a viscoelastic continuous phase, Flumerfelt [10] and Tavgac [11] formulated an expression by adopting the Bird-Carreau viscoelastic model as rheological representation.

In order to investigate the effect of fluid elasticity on deformation of a viscoelastic droplet suspended in another viscoelastic medium under a steady elongational flow, Chin and Han [12, 13] obtained the first-order solution for predicting the droplet shape, using the Coleman-Noll second-order fluid. They also carried out a hydrodynamic stability analysis for the breakup, using the classical Jeffreys model. Although they made theoretical attempts to predict the deformation and breakup of viscoelastic fluid droplets, their work has not yet led to a general understanding of the phenomenon because their theoretical development has severe limitations. Recently, for a viscoelastic system, the problem of droplet deformation and breakup was investigated by Wu [14] for blends of nylon and polyester as the matrix and ethylene-proylene rubbers as the dispersed phase, processed by co-rotating twin screw extrusion at constant dispersed phase volume fraction. This system is quite different from Taylor's in many respects, i.e., both dispersed and continuous phases are viscoelastic, and the strain field is a complex combination of nonuniform, transient shear and elongational fields. More recently, Serpe, Jarrin and Dawans [15] modified the Wu's expression [14], based on the influence of the dispersed phase concentration and blend viscosity on blend morphology.

The objectives of this study are to characterize low density polyethylene/nylon 6 blends from a rheological point of view, and to study the morphology of the minor phase as a function of composition. The rheological properties of two-phase polymer systems are investigated in oscillatory shearing flow and in elongational flow fields. The effect of the viscosity ratio on the phase size/composition dependence and the interfacial and rheological effects on the dispersion process will also be discussed.

2. Experimental

2.1. Materials and Blend Preparation

Four low density polyethylenes (PE-1, PE-2, PE-3, PE-4) with different molecular weights and a nylon 6 (N6) were used. The characteristics of these polymers are summarized in Table 1. The polymers were blended by using a screw extruder with a static mixer. A 30 mmϕ extruder was used in order to feed and mix the material. A static mixer (Sam Hwa MFG. Co.) with seven mixing elements was attached to improve mixing efficiency. The polymer blends were prepared in composition ranges defined in Table 2. All the PE/N6 blends were blended at 260℃. In order to keep constant throat pressures and throughputs for all the blends, screw speeds were changed according to the types of polyethylenes.

2.2. Rheological Measurement

2.2.1. Dynamic Flow Properties

A Rheometrics Dynamic Spectrometer (RDSII,

Table 1. Characteristics of polymers studied

Material	Supplier	MI[a]	Density (g/cm^3)	$\bar{M}n^b$	$\bar{M}w^b$	$\bar{M}w/\bar{M}n$
PE-1	Hanyang Chemical	45	0.915	21,600	172,800	8.0
PE-2	〃	24	0.915	23,700	218,000	9.2
PE-3	〃	8.0	0.918	23,900	258,100	10.8
PE-4	〃	0.25	0.921	28,000	261,000	9.3
N6	Tongyang Nylon	—	1.143	19,700	37,500	1.9

[a] 190℃ /2,160 g/10 minutes

[b] $\bar{M}n$ and $\bar{M}w$ of LDPE's were determined by GPC. $\bar{M}n$ of NY6 was determined by end group analysis. $\bar{M}w$ of NY6 was calculated by the formula $\bar{M}w=53788\ (\sqrt{R.V.}-1)$ where the R.V. is the relative viscosity measured on a 1% w/v solution in 96% sulphuric acid at 25℃.

Table 2. Blend systems investigated

System	Compositions (wt%/wt%)	Channel apparent shear rate (s^{-1})[a]
Polyethylene-1/Nylon 6 (PE-1/N6)	90/10, 70/30, 50/50, 35/65, 30/70, 10/90	100
Polyethylene-2/Nylon 6 (PE-2/N6)	90/10, 70/30, 60/40, 50/50, 40/60, 35/65, 30/70, 10/90	50
Polyethylene-3/Nylon 6 (PE-3/N6)	90/10, 70/30, 50/50, 45/55, 30/70, 10/90	20
Polyethylene-4/Nylon 6 (PE-4/N6)	90/10, 70/30, 60/40, 50/50, 30/70, 10/90	10

[a] Values calculated by the formula $\dot{\gamma}_a=\pi dn/60h$ where d, n, and h are barrel diameter, screw speed (rpm), and minimum channel depth, respectively.

Model 7700) was used to measure the complex viscosity, η^*, and the storage modulus, G', as a function of frequency at 260℃. The experiments were carried out in the dynamic mode in parallel plate geometry at a strain of 10% and a gap of 2.0 mm. The RDS measurements were performed under dry nitrogen.

2.2.2. Elongational Flow

The apparatus used (Capirograph) is essentially a lab-scale melt spinning equipment, consisting of a reservoir section with a capillary, a tensiometer, and a take-off device. The capillary used had a diameter of 1.0 mm, an L/D ratio of 20. An isothermal chamber (14-cm long) was attached to the capillary in order to keep the temperature of the molten threadline nearly equal to that of the melt. A camera (PENTAX-MX, Asahi) was used to take pictures of the threadlines. The temperature of the reservoir was kept to be 230℃ and the residence time was 1 minute to minimize the coalescence of the dispersed phases. At that time, the temperature of the isothermal chamber was 210± 5℃. The diameter profile of the fiber inside the isothermal chamber was recorded and measured both by a laser beam and by taking pictures through the glass window of the chamber. The laser beam was placed 10 to 20 mm distant from the capillary. In order to project pictures on the screen, a projector (ELMO OPAQUE PROJECTOR) was used. The magnitude was about 20. The thread tension was measured at 650 mm from the bottom of capillary where the threadline solidified. The actually measured tension for PE-1/N6, PE-2/N6 and PE-3/N6 blends were determined at take-up speeds of 20 m/min, while the data for PE-4/N6 were measured at take-up speeds of 10 m/min because filament breakage occurred at the speeds of 20 m/min. The extrusion velocity V_0 was

0.91 m/min.

2.3. Morphological Analysis

A scanning electron microscope (type JEOL 35 CF) was used to examine samples and to verify the morphology. The blended samples were microtomed to create a plane face using an ultramicrotome equipped with a glass knife. The samples stretched by spinning were fractured under liquid nitrogen and the fracture surfaces were examined. In order to observe fiber formation or fibrillation of dispersed phases, the stretched samples were extracted by using toluene or formic acid. Extraction in toluene would remove the polyethylene and leave the nylon 6. Extraction in formic acid would remove the nylon 6 and leave the polyethylene. The characteristics of the extracted filaments were also investigated.

3. Results and Discussion

3.1. Rheological Properties

In Fig. 1, complex viscosity (η^*) is plotted versus angular frequency (ω) for the four commercial polyethylene samples and nylon 6 at 260℃. The nylon 6 sample exhibits nearly Newtonian flow behavior and shows a higher viscosity than PE-1, PE-2, and PE-3 over the frequency range observed. Fig. 2 shows that the elastic property represented by the storage modulus (G′) is similar for four LDPE's and the LDPE's exhibit higher storage modulus than nylon 6 over all the range of shear stresses (τ).

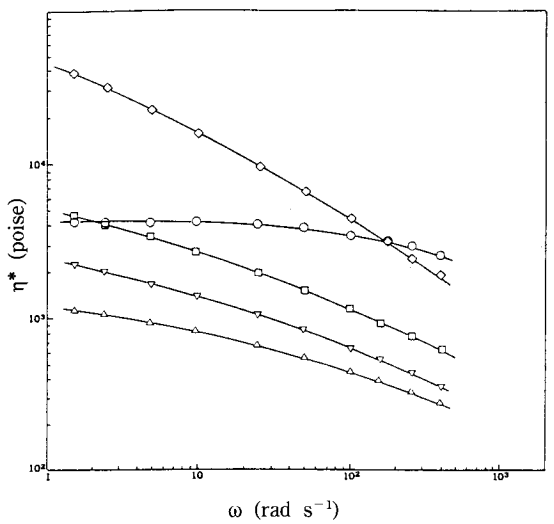

Fig. 1. η^* versus ω for the homopolymer samples: PE-1 (△), PE-2 (▽), PE-3 (□), PE-4 (◇) and N6 (○).

3.2. Analysis of Dispersion Process

3.2.1. Dependence of Phase Size on the Blend Compsition

SEM photomicrographs of the fracture surfaces of PE-1/N6 extrudates produced in this work are shown in Fig. 3. It is seen that at high polyethylene content levels the nylon 6 forms the dispersed phase and at high nylon 6 contents the polyethylene is the dispersed pahse. At intermediate compsoitions, co-continuous phases are obtained. The phase dimensions are in the range of 3 to 45 μm. The number average dispersed phase dimensions have been determined by observing a blend containing 80 to 250 dispersed globules for

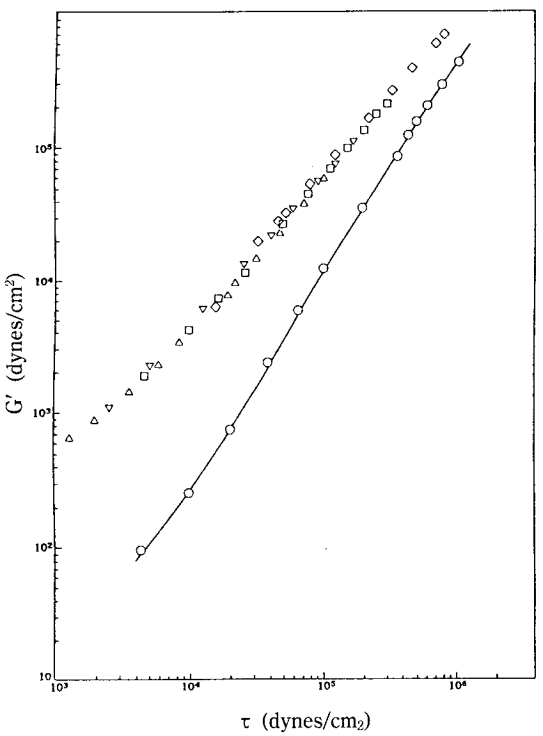

Fig. 2. G′ versus τ for the homopolymer samples: PE-1 (△), PE-2 (▽), PE-3 (□), PE-4 (◇) and N6 (○).

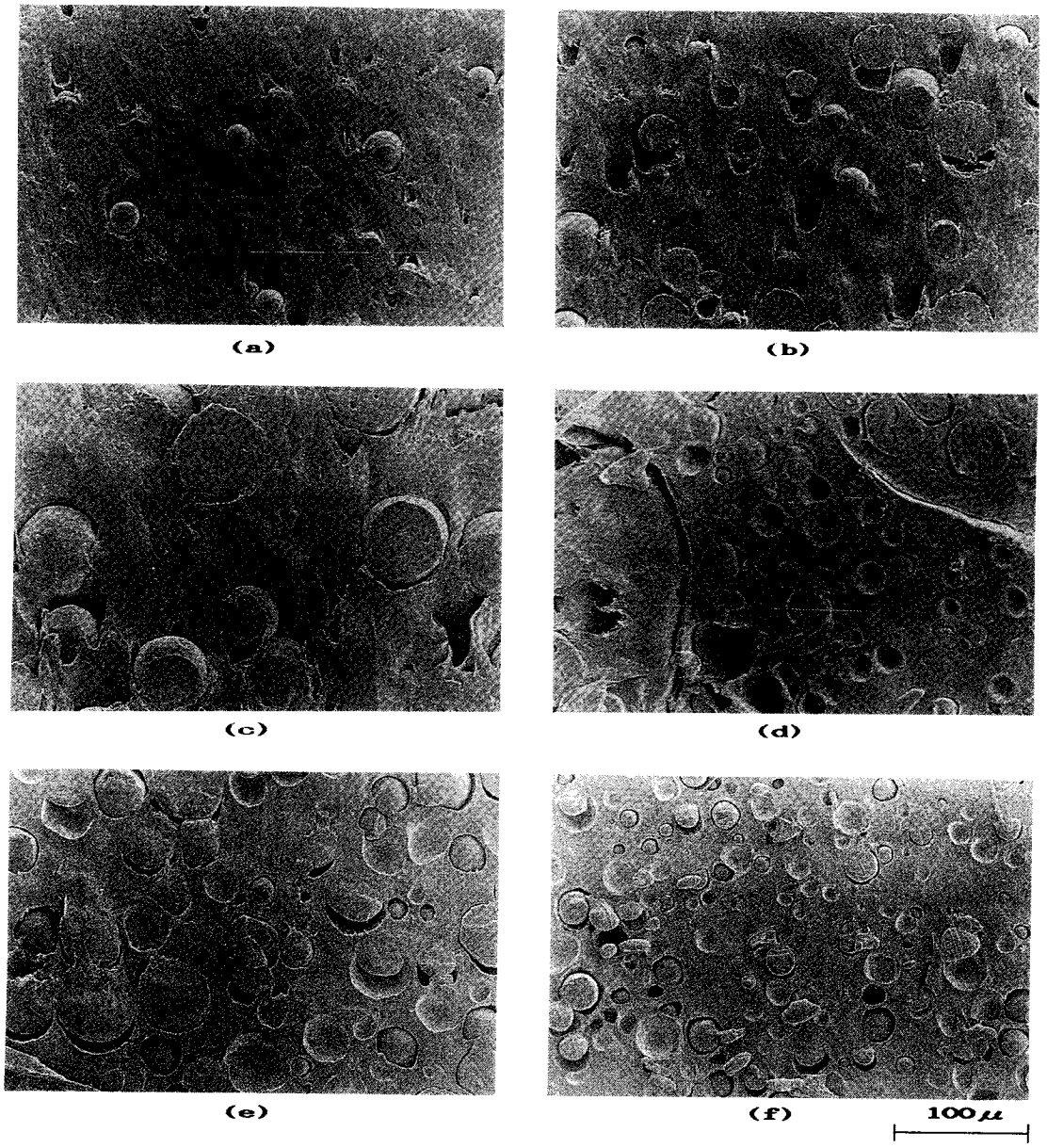

Fig. 3. SEM photomicrographs of PE-1/N6 blends: (a) 90/10, (b) 70/30, (c) 50/50, (d) 35/65, (e) 30/70, (f) 10/90, (wt%/wt%).

each system. These results are plotted versus nylon 6 content in Fig. 4. This shows the dependence of the number average diameter with composition. The composition dependence for the blend is characterized by the curves which display asymptotic behaviour at intermediate concentrations. At low nylon 6 concentrations, there is a gradual increase of phase dimensions with increasing nylon 6 contents.

3.2.2. Dual-phase Continuity

Recently, a semi-empirical expression was proposed to predict the point of co-continuous phases based on the viscoisty ratio [16]:

$$\eta_1(\dot{\gamma})/\eta_2(\dot{\gamma}) \sim \Phi_1/\Phi_2 \quad (1)$$

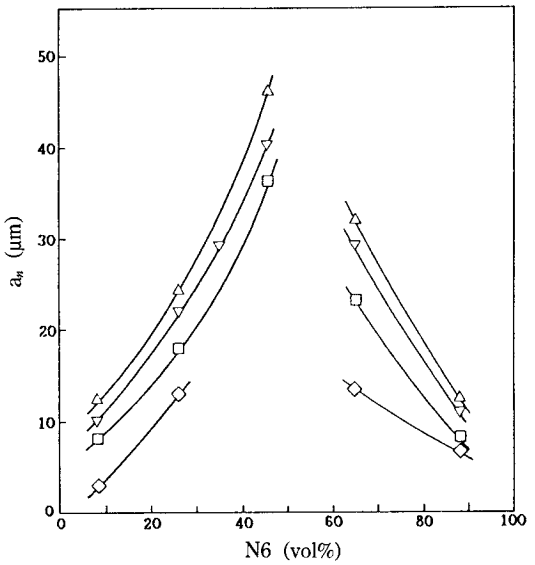

Fig. 4. Dependence of phase size on composition for blends: PE-1/N6 (△), PE-2/N6 (▽), PE-3/N6 (□), PE-4/N6 (◇).

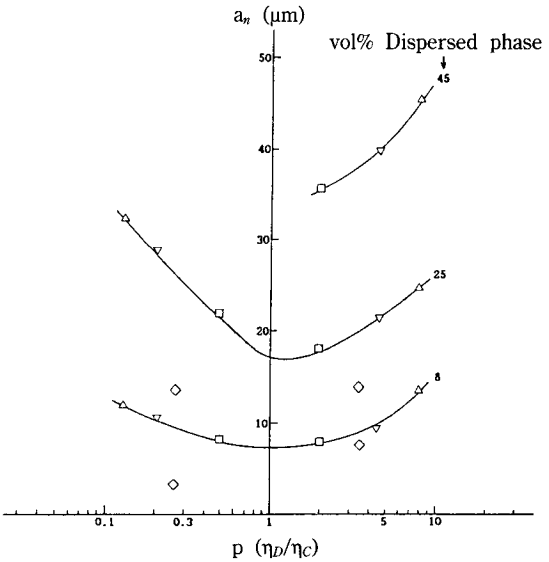

Fig. 5. Dependence of number-average diameter of dispersed phase on the viscosity ratio: PE-1 /N6 (△), PE-2/N6 (▽), PE-3/N6 (□), PE-4/N6 (◇).

Table 3. Concentration for dual-phase continuity

	Φ_{N6} (pred.)	Φ_{N6} (obs.)
PE-1/N6	0.88	0.60
PE-2/N6	0.82	0.55~0.60
PE-3/N6	0.67	0.50
PE-4/N6	0.21	0.35

where Φ's designate the volume fraction of a two phase system. According to Eq. 1, the region of dual-phase continuity would be theoretically predicted (Table 3). Using the approximate Cox-Merz rule, $\eta^*(\omega)$ may replace $\eta(\dot{\gamma})$ in Eq. 1 [17]. The predicted values are calculated under the processing conditions previously described in Table 2 and Fig. 1. Experimentally, however, co-continuous phases are observed with a large deviation. These experimental results may be supported by those of Favis and Chalifoux [18], who observed co-continuous structures at 40~50 vol% for polypropylene/polycarbonate blends, compared with the 68~87 vol% predicted by Eq. 1. We can also see the difference between the predicted and observed values for dual-phase continuity in this study. This may be due to the storage modulus of polyethylene being larger than that of nylon 6 for PE-1/N6, PE-2/N6, and PE-3/N6 blends. However, for PE-4/N6 blends processed with very high shear stresses, the condition for dual phase continuity can be predicted fairly accurately using the relation because the storage moduli of PE-4 and N6 may be almost the same at high shear stress. Therefore, the morphological data concerning the region of co-continuous phases appear to be related to the relative elasticity of the components in the blend as well as viscosity ratio for these systems.

3.2.3. Interfacial and Rheological Effects

Fig. 5 shows plots of the number-average particle diameter (a_n) versus the viscosity ratio ($p=\eta_D/\eta_C$, where η_C and η_D are the continuous and dispersed phase viscosities, respectively) at the effective shear rate of the extruder and the extruder melt temperature. For all blends obtained we note that the number average diameter of the dispersed phase (N6 or PE) is a function of the relative viscosities as well as the concentration of the dispersed phase. It seems that the influence of the mixing conditions on PE/N6 blend morphology may be described by Wu's expression [14] or Se-

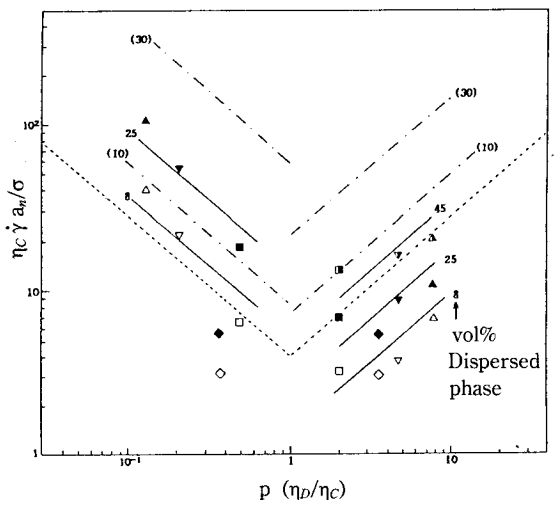

Fig. 6. Dimensionless curves of Weber number versus viscosity ratio: PE-1/N6 (△, ▲, ◭), PE-2/N6 (▽, ▼, ▽), PE-3/N6 (□, ■, ◨), PE-4/N6 (◇, ◆).
--- Wu's curve, -·- Serpe-Jarrin-Dawans curves.

rpe *et al.*'s modification [15].

The critical Weber number ($\eta_C\dot{\gamma}a_n/\sigma$) is plotted versus the viscosity ratio p in Fig. 6, over a wide range of composition. In this study, we used 10.7 mN/m for the interfaical tension (σ) of the PE/N6 system, measured by means of the spinning drop method at 250℃ [19]. For the same compositions of blends, the data points fall nearly on straight lines which are parallel to Wu's curve. Thus, in this case it appears that the dispersed phase concentration is an independent parameter of blend components for the same blending process and the average diameter of particles increases with the dispersed phase concentration. Wu [14] proposed that there was a critical value of the Weber number below which particle deformation would no longer occur, and therefore there was a critical particle size determined by the rheological effects. At that point the emulsion system achieved the minimum interfacial area possible by a critical average particle size of the dispersed phase for a fixed composition. Therefore, if one changes the mixing conditions or the system composition, the system follows a V-shaped curve parallel to Wu's curve according to Serpe *et al.*'s modifications [15]. In Figs. 5 and 6, there are deviations from the curves or straight lines for PE-4/N6 blends. Such deviations may be due to high pressures applied in preparing the blends with very high viscosity PE-4.

3.3. Deformation in Elongational Flow

Elongation of droplets can take place in a shear field with a non-uniform velocity profile. However, more efficient is the extensional stress. In other words, drop breakup occurs much more easily in an elongational field than in a shear field. Extensional flow was also found to have a stabilizing effect on the breakup of liquid threads. At high extensional rates, very small diameter thread could be maintained before the final breakup occurs [20].

In the fiber spinning process, a rheological property of direct relevance is elongational viscosity. Using the melt spinning process, the elongational viscosity can be determined by

$$\eta_E = \frac{F/A(x)}{dV(x)/dx} \tag{2}$$

where η_E is the elongational viscosity, F, the force required to deform a threadline, x, the direction of the fiber streching, A(x), the corss sectional area of a threadline at position x and dV(x)/dx or $\dot{\gamma}_E$, elongation rate at position x. In the melt spinning process, the forces involved in deforming a threadline are: the rheological force (F_{rheo}), gravitational force (F_{grav}), drag force (F_{drag}), and inertia force (F_{inert}). The overall force balance around a threadline may be written as

$$F_{rheo} = F_L + F_{grav} - F_{drag} - F_{inert} \tag{3}$$

The gravitational force may be determined from

$$F_{grav} = \int_x^L \rho g \pi/4\, D(x)^2\, dx \tag{4}$$

where g is the gravitational constant, ρ, the fluid density and D(x), the thread diameter at position x. In the case where the take-up velocity is very low, inertia and air drag forces are negligibly small [21]. With the measured tension (F_L) and

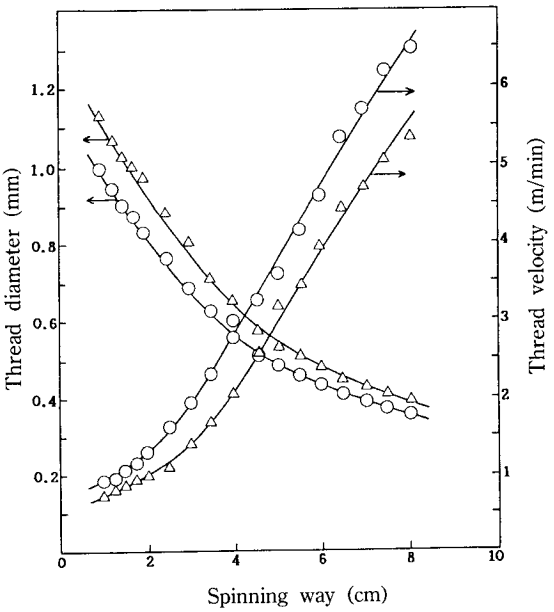

Fig. 7. Profiles of thread diameter and thread velocity for PE-1 (△) and N6 (○).

the calculated values, F_{rheo} can be calculated, which will then permit one to determine the elongational viscosity from Eq. 2.

Fig. 7 shows the profiles of the thread diameter and thread velocity along the spinning way for the PE-1 and N6. The velocity profile is determined by use of the equation of continuity. Apparent elongational viscosity-elongation rate data for four polyethylenes and nylon 6 are shown in Fig. 8. For polyethylenes, the η_E values increase with elongation rate. In particular, the value of PE-4 increases strikingly with elongation rate. For nylon 6, the η_E value increases slightly with elongation rate.

From SEM photomicrographs of the fiber samples of PE/N6 blends at a stretch ratio of 11, the number-average fibril dimensions have been determined using 60 to 300 dispersed fibrils for each system. The values so determined are summarized in Table 4. Fiber formation is observed after extractions of LDPE in toluene or nylon 6 in formic acid. Fig. 9 shows SEM photomicrographs of the longitudinal section of toluene- or formic acid-extracted fibers. The values of the average fibril

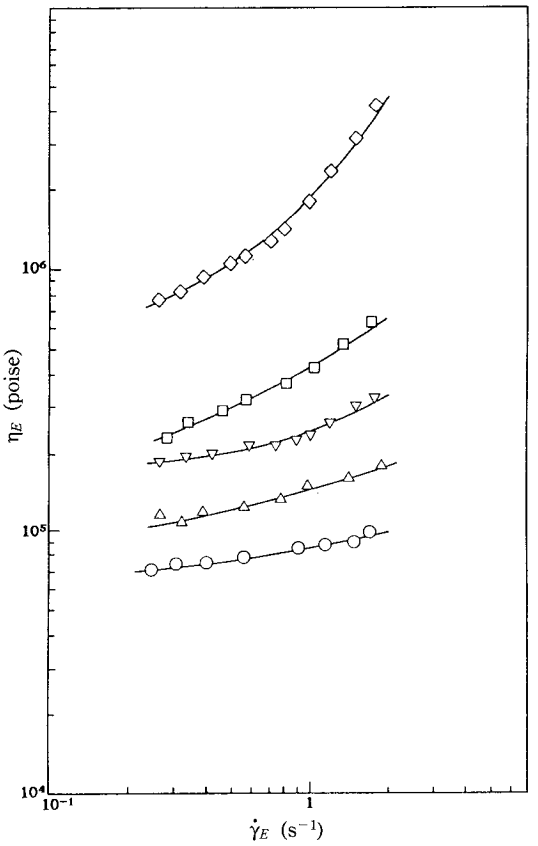

Fig. 8. η_E versus $\dot{\gamma}_E$ for the homopolymer samples: PE-1 (△), PE-2 (▽), PE-3 (□), PE-4 (◇) and N6 (○).

lengths and aspect ratios of the nylon 6 or LDPE fibrils calculated at take-up speeds of 10 m/min ($V_L/V_0=11$), assuming no breakup of the dispersed phase during the spinning process, are given in Table 5. The assumption of no breakup may be valid. As discussed, Rumscheidt and Mason [5, 6] and Lee [20] observed that very fine diameter threads were made before the breakup was observed in extensional flow. Shimizu *et al.* [22] also observed that the dispersed fibers could be made thinner with higher take-up speeds.

On the other hand, Han and Kim [23] observed that the deformation of droplets in an extensional flow was possible if $\eta_{E,D}/\eta_{E,C}<1$ for polystyrene/HDPE blends. In other words, when the dispersed phase has an elongational viscosity lower than the continuous phase, the suspended droplets can be

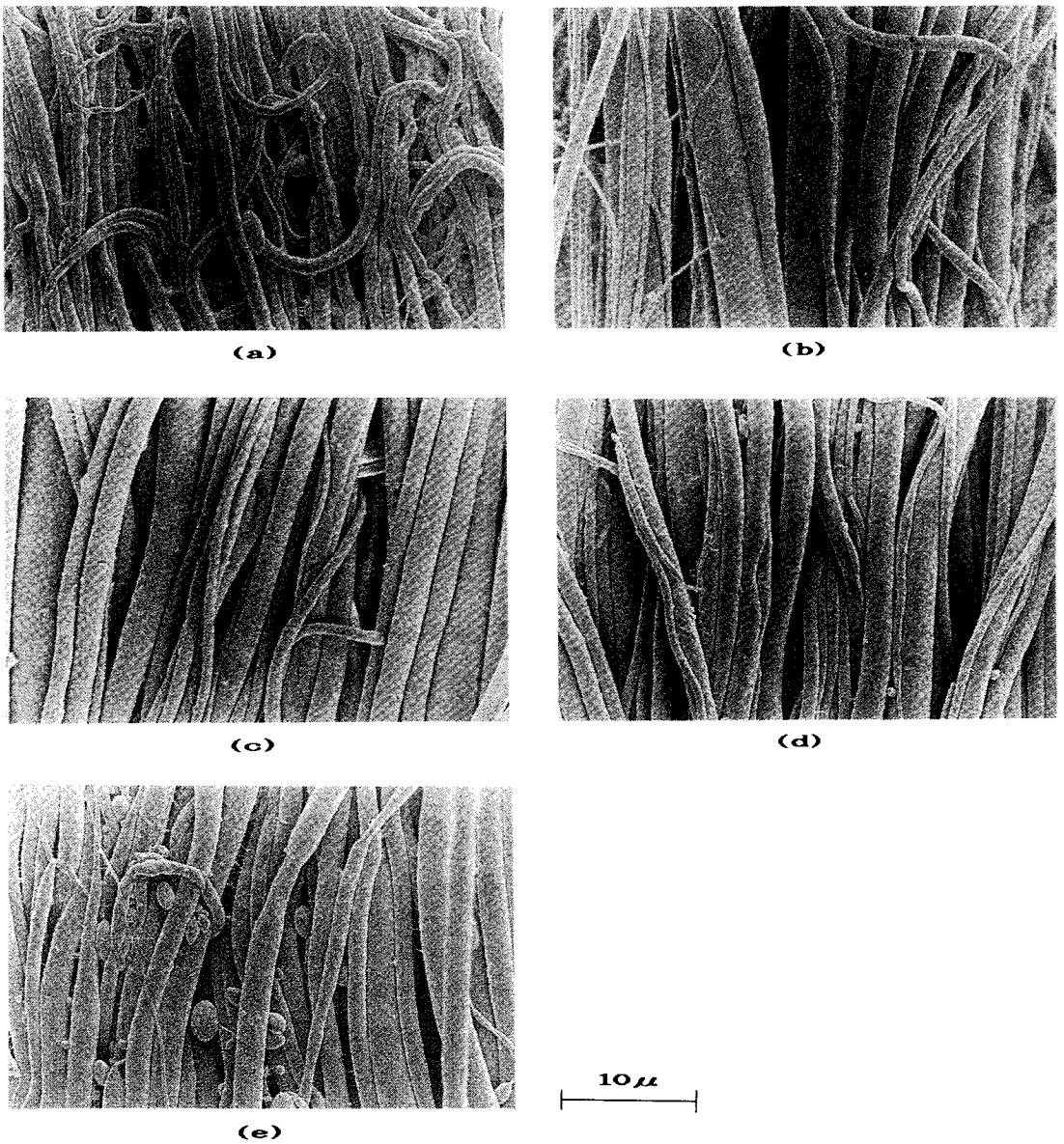

Fig. 9. SEM photomicrographs of longitudinal section of solvent-extracted PE-1/N6 blend melt-spun fibers (V_L/V_0 =11): (a) 90/10, (b) 70/30, (c) 50/50, (d) 30/70, (e) 10/90, (wt%/wt%).

expected to elongate much more easily. In the opposite situation, the suspended droplets would elongate much less than the continuous phase. In that case, it should be noted that both polystyrene and HDPE show tension-thinning. However, for the PE/N6 blends investigated in this work, the deformation of droplets is different from Han and Kim's result. In all cases, the dispersed phase (N6 or PE) elongates with stretch ratios irrespective of the elongational viscosity ratio of two homopolymers. For only the PE-4/N6 blends (30/70, 10/90 blends) with a very high η_E value, the dispersed PE droplets are less elongated, and thus the fibrils have low aspect ratios.

Table 4. Number-Average fibril diameter by spinning process

System	Stretch ratio (V_L/V_0)	Composition (PE/N6, μm)				
		90/10	70/30	50/50	30/70	10/90
PE-1/N6	11	1.0	1.9	2.5	2.2	1.4
	22	0.6	1.1	1.4	1.2	1.0
PE-2/N6	11	1.0	1.7	2.2	2.1	1.2
	22	0.6	1.1	1.4	1.4	0.7
PE-3/N6	11	0.9	1.4	2.0	1.7	1.1
	22	0.5	0.8	1.2	1.3	0.8
PE-4/N6	11	0.5	0.8	2.3	2.8	3.2

Table 5. Dimensions of nylon 6 or LDPE fibrils

System	Calculated dimension	Composition (PE/N6)				
		90/10	70/30	50/50	30/70	10/90
PE-1/N6	length (mm)	1.30	2.95	10.52	4.56	0.60
	aspect ratio ($\times 10^{-2}$)	13.02	16.40	42.07	20.71	4.30
PE-2/N6	length (mm)	0.57	2.49	8.68	3.73	0.67
	aspect ratio ($\times 10^{-2}$)	5.72	14.65	39.47	17.74	5.57
PE-3/N6	length (mm)	0.56	2.02	8.04	2.81	2.8
	aspect ratio ($\times 10^{-2}$)	6.23	14.41	40.19	16.51	2.56
PE-4/N6	length (mm)	0.09	1.98	–	0.20	0.03
	aspect ratio ($\times 10^{-2}$)	1.75	3.13	–	0.71	0.10

It is a well-established fact that the tension-thickening group, which is a flexible polymer, shows less aligning and more stretching in extensional flow fields and the tension-thinning group, which is less flexible (rod-like), shows more aligning and less stretching [24, 25]. Both nylon 6 and LDPE investigated in this study exhibit tension-thickening. It may be, therefore, concluded that the dispersed fibrils of nylon 6 or LDPE can be made much thinner by increasing the stretch ratio, irrespective of the elongational viscosity ratio of the dispersed to continuous phases. For the 70/30 (PE/N6) blends, the average diameters of the nylon 6 fibrils obtained at take-up speeds of 10 m /min are measured to be 0.8~1.8 μm and the average fibril lengths are estimated to be 2~3 mm. The ultrafine fibrils obtained in this manner have aspect ratios reaching 10^4. For the 30/70(PE/N6) blends, the average diameters of the LDPE fibrils are measured to be 1.7~2.8 μm and the average fibril lengths were estimated to be 0.2~4.5 mm. The ultrafine fibrils have aspect ratios reaching 10^2~10^4. It can be also seen in Table 5 that the aspect ratios become larger with increasing the content of the dispersed phases. This trends may fit to the deformation equation of Choi and Schowalter [9].

4. Conclusions

The deformation and breakup processes of dispersed phases in the immiscible binary blend systems of polyethylene and nylon 6 under shear flow and elongational flow fields have been studied.

The formation of a dispersed phase during melt blending with a single screw extruder and a static mixer shows composition dependence. The analysis of the PE/N6 blend morphology reveals the size of the minor phase to display a strong increase in the dispersed phase size when the minor component concentration is increased, especially

in the vicinity of dual-phase continuity. The experimental results of the dispersion can be described by a curve relating the Weber number to the viscosity ratio. A shift in the region of dual-phase continuity is also observed for blends of different viscosity ratios. The morphological data concerning the region of co-continuous phase appear to be related to the relative elasticity of the components as well as the viscosity ratio.

The ultra-fine fibril formation is observed in a uniaxial elongational flow. For the 70/30(PE/N6) blends, the average diameters of the nylon 6 fibrils obtained at take-up speeds of 10 m/min are 0.8~1.8 μm and the average fibril lengths, 2~3 mm. For the 30/70(PE/N6) blends, the average diameters of the LDPE fibrils are 1.7~2.8 μm and the average fibril lengths, 0.2~4.5 mm. Therefore, very thin diameter fibrils of nylon 6 or LDPE can be obtained, irrespective of the elongational viscosity ratio of the dispersed to continuous phases.

References

1. G.I. Taylor, *Proc. Roy. Soc. (London)*, **A146**, 501 (1934).
2. G.I. Taylor, *ibid.*, **A138**, 41 (1932).
3. W. Bartok and S.G. Mason, *J. Colloid Sci.*, **13**, 293 (1958).
4. W. Bartok and S.G. Mason, *ibid.*, **14**, 13 (1959).
5. F.D. Rumscheidt and S.G. Mason, *ibid.*, **16**, 210 (1961).
6. F.D. Rumscheidt and S.G. Mason, *ibid.*, **16**, 238 (1961).
7. H.J. Karam and J.C. Bellinger, *Ind. Eng. Chem. Fundam.* **7**, 576 (1968).
8. H.P. Grace, *Chem. Eng. Commun.*, **14**, 225 (1982).
9. S.J. Choi and W.R. Schowalter, *Phys. Fluids*, **18**, 420 (1975).
10. R.W. Flumerfelt, *Ind. Eng. Chem. Fundam.*, **11**, 312 (1972).
11. T. Tavgac, Ph.D. Dissertation, Univ. of Houston, Houston, Texas, 1972.
12. H.B. Chin and C.D. Han, *J. Rheol.*, **23**, 557 (1979).
13. H.B. Chin and C.D. Han, *ibid.*, **24**, 1 (1980).
14. S. Wu, *Polym. Eng. Sci.*, **27**, 335 (1987).
15. G. Serpe, J. Jarrin and F. Dawans, *ibid.*, **30**, 553 (1990).
16. I.S. Miles and A. Zurek, *ibid.*, **28**, 796 (1988).
17. R.B. Bird, R.C. Armstrong and O. Hassager, "Dynamics of Polymeric Liquids", Vol. 1, John Wiley & Sons, New York, 1977.
18. B.D. Favis and J.P. Chalifoux, *Polymer*, **29**, 1761 (1988).
19. J.J. Elmendorp and G. De Vos, *Polym. Eng. Sci.*, **26**, 415 (1986).
20. W.K. Lee, Ph.D. Dissertation, Univ. of Houston, Houston, Texas, 1972.
21. D. Acierno, J.N. Dalton, J.M. Rodriguez and J.L. White, *J. Appl. Polym. Sci.*, **15**, 2395 (1971).
22. J. Shimizu, N. Okui, T. Yamamoto, M. Ishii and A. Takaku, *Sen-I Gakkaishi*, **38**, T-1 (1982).
23. C.D. Han and Y.W. Kim, *J. Appl. Polym. Sci.*, **18**, 2589 (1974).
24. H.A. Barnes, J.F. Hutton and K. Walters, "An Introduction to Rheology", Elsevier, 1989.
25. Y. Ide and J.L. White, *J. Appl. Polym. Sci.*, **22**, 1061 (1978).